INTERNATIONAL JOURNAL OF CONSERVATION SCIENCE

ISSN: 2067-533X Volume 14, Issue 2, April-June 2023: 599-616 www.ijcs.ro

DOI: 10.36868/IJCS.2023.02.15

# CHARACTERIZATION OF CONSTRUCTION MATERIALS OF THE HISTORIC STRUCTURES IN HISTORIC CAIRO: A CASE STUDY

Ahmed ELYAMANI[1], Ahmad REDA[2,*],
Mahmoud ABDEL-HAFEZ[1], Sherif A. MOURAD[2], Maha M. HASSAN[2]

[1] Archaeological Conservation Department, Faculty of Archaeology, Cairo University – 1 Gamaa Street, Giza, Egypt
[2] Department of Structural Engineering, Faculty of Engineering, Cairo University – 1 Gamaa Street, Giza, Egypt

***Abstract***

*The paper presents a comprehensive experimental programme aimed at the characterization of the construction materials of the Fatima Khatun Mausoleum in Historic Cairo, built in the 13th century. The mausoleum reached an advanced state of degradation and, in short, turned into a garbage dump. A joint research project between Egypt and the United Kingdom was launched, aiming at its conservation in general and proposing guidelines for the management and conservation of historic Cairo. Representative samples were collected from the limestone, the historic and new bricks used in a previous restoration, the mortar, and the salt. The physical, chemical, petrographic, and mechanical properties were determined experimentally. It can be claimed that the construction materials of the mausoleum were characterised to a good extent, which will help in any future intervention when choosing new limestone, mortar, and bricks to select compatible materials with the historic ones.*

***Keywords**: Historic Cairo; Historic Masonry; XRD, SEM-EDX; Compressive Strength*

## Introduction

Historic Cairo is rich with more than 600 historic structures; some of them date back more than one thousand years; therefore, it was declared a UNESCO World Heritage Site in 1979. Although there is an appreciated effort from the authorities in charge to preserve this historic site from damage, there are many historic structures suffering from misuse, neglect, rising groundwater levels, and many other damage causes. For that reason, there is a persistent need to carry out field studies on the historic Cairo's structures, which are undergoing continuous deterioration.

The Egyptian state makes considerable efforts to preserve historic Cairo to the extent possible. In specific, after the 1992 earthquake that hit Cairo and resulted in more than 560 deaths and thousands of injuries [1], Historic Cairo Islamic buildings were badly affected, and 140 were damaged and in danger of collapse; in addition, several minarets were tilted [1]. Therefore, a big restoration project was launched in 1998 and is still active. The main work was conducted between 2002 and 2006, during which more than 100 historic structures were restored [2]. However, and unfortunately, efforts are still not capable of maintaining the large number of historic structures that Historic Cairo has.

It is sad to say that there are several examples of neglected historic structures that are suffering from very harsh surrounding conditions and are nowadays considered garbage dumps, and the case study of this research is one of them. This is a result of many reasons, among them

* Corresponding author: reda.ahmad@cu.edu.eg

the limited available budget allocated for restoration projects and the large number of historic structures in need of intervention. This problem is an optimisation one. *D.A. Saad et al.* [3] proposed a fund-allocation optimisation model in which several historic structures are considered compotators to win a part of the allocated restoration budget. The historic structures' restoration priority was determined to maximise the socioeconomic benefits and structural physical performance while minimising further damage.

Some other reasons are the lack of periodic maintenance, the absence of the application of new monitoring technology, rising groundwater levels, and the absence of waste management plans, among others. For this reason, there is a need for more research projects on the topic of the conservation of historic structures in Cairo. Therefore, the research project is called "Interdisciplinary Approach for the Management and Conservation of the UNESCO World Heritage Site of Historic Cairo. Application to Al-Ashraf Street" [4] was launched with the aim of proposing guidelines for better conservation and management plans for Historic Cairo. A part of the site was chosen as a case study, which is Al-Ashraf Street, which contains eight historic structures, among them the Mausoleum of Fatima Khatun, the case study of this paper.

It is well known that the first step towards a comprehensive conservation plan is gathering enough information about the construction materials, aside from the history, the architectural documentation, and the photographic and video documentation, among other interconnected activities aiming at maximising the level of knowledge about the considered historic structure [5, 6].

The characterization of the construction materials of historic structures could involve several in-situ and laboratory investigations. For its specific nature as historic materials, it is recommended to employ only non-destructive or at most semi-destructive techniques [7].

To mention some, the single and double flat jack tests [8] aim at determining regular masonry compressive strength and modulus of elasticity. For irregular masonry, the tube jack test is under development and formulation [9]. Laboratory testing in compression and shear of historic masonry [10-12]. Some other non-destructive techniques include: GPR [13, 14], ultrasonic pulse velocity [15], thermography [16], X-ray Diffraction (XRD) [17-20], and Scanning Electron Microscopy with Energy Dispersive X-Ray Analysis (SEM-EDX) [21-25].

In this research, the characterization of the construction materials of the Mamluk Mausoleum of Fatima Khatun, dating back to the $13^{th}$ century, has been performed. This is the first step to gaining sufficient knowledge about this structure to propose a proper conservation plan because it is currently turned into a garbage dump (Fig. 1). It suffers from serious deterioration, neglect, and the raising of groundwater to more than a metre above its ground level and is now, with great regret, a garbage dump. It was constructed from limestone and brick masonry.

Representative samples were collected from the limestone, the historic and new bricks used in a previous restoration, the mortar, and the salt. The physical properties of the bulk specific weight, the porosity, and the water absorption were determined experimentally for the limestone, the old, and the new bricks. The uniaxial compression test was carried out on old and new brick cubes and on cylinders and cubes taken from the limestone. Comparative studies were carried out with other results obtained from the limited available literature on testing historic stone and brick in historic Cairo. The aim was to check the results obtained in this research and to take a step towards a database involving guide values for the compressive strength of Historic Cairo's used stone and brick.

The polarised optical microscope was employed to investigate the petrography of the limestone and the old and new bricks. Samples from the limestone, the old and new bricks, the mortar, and the salt were examined using X-Ray Diffraction (XRD) and a Scanning Electronic Microscope provided with an Energy Dispersive X-Ray Analyzer (SEM-EDX). From this comprehensive set of tests and analyses, it can be claimed that the construction materials of the Fatima Khatun Mausoleum were characterised to a good extent. This will help in any future intervention when choosing new limestone, mortar, and bricks to choose compatible materials with the historic ones. Also, it will help with the next structural assessment tasks.

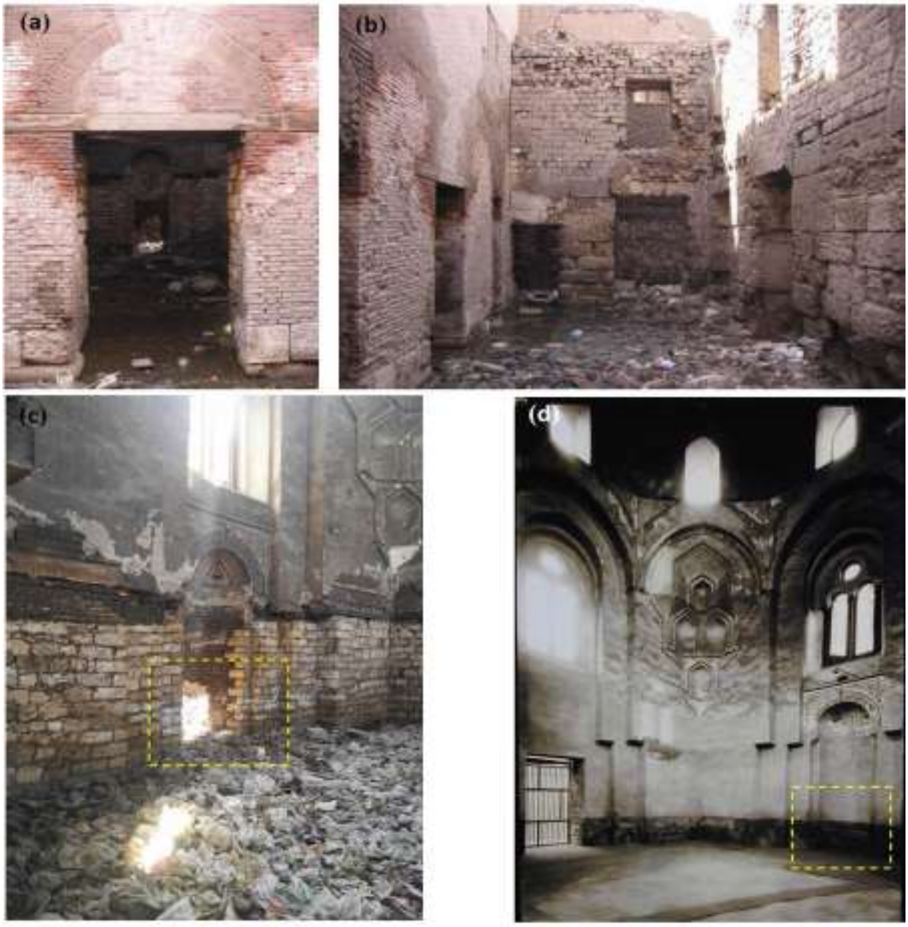


**Fig. 1.** Current situation of Fatima Khatun Mausoleum: (a) high groundwater penetration by capillarity in masonry walls; (b) local damages and accumulation of groundwater and garbage; (c) garbage dump inside the mausoleum and partial collapse of a wall; (d) historic photo showed no deterioration (source: Creswell collection) [26])

***Historical Background***

This mausoleum was a part of a complex madrasa (school) built in 1284 A.D. by Al-Mansour Qalawun (8$^{th}$ Sultan of the Bahri Mamluk Sultan) for his wife Fatima Khatun. Qalawun took the sultanate for about 10 years, from 1279 to 1290 A.D. [27]. Both Fatima Khatun and her son al-Malik al-Salih Al'a El-Din were buried in this mausoleum in 1283 A.D. and 1288 A.D., respectively [27]. The architect was Amir Singer al-Shok'ai, who was also the architect of the famous Qalawun complex in al-Moaz Street in historic Cairo. The madrasa was severely damaged, and what is left now is only the mausoleum, the entrance, the minaret, and a part of the front hall [27].

***Description***

The Fatima Khatun complex is composed of the mausoleum, the entrance, the hall, and the minaret (Fig. 2). The entrance, with a width of about 3.5m and a height of 7m, is located on the northwest side, looking at al-Ashraf Street, which is considered an extension of al-Moaz Street in Historic Cairo. To the right of the entrance, there is a hall of about 8.1m in length and 2.7m in width. It was once covered by a vault that had collapsed. The minaret has a rectangular cross section with dimensions of 6.1m length by 5.8m width and a total height of about 21.2m. At the minaret top, there was once a group of columns supporting a small dome, but unfortunately, they all collapsed. The mausoleum itself has a square plan with a side length of about 14.3m from outside and 10.4m from inside, meaning that the walls are two metres thick. The walls are constructed from several courses of limestone masonry at the base, and then the full height is brick masonry. The square plan is then converted into an octagon. The mausoleum was once covered by a dome that had collapsed. Nowadays, it is protected by a wooden roof [27-29].

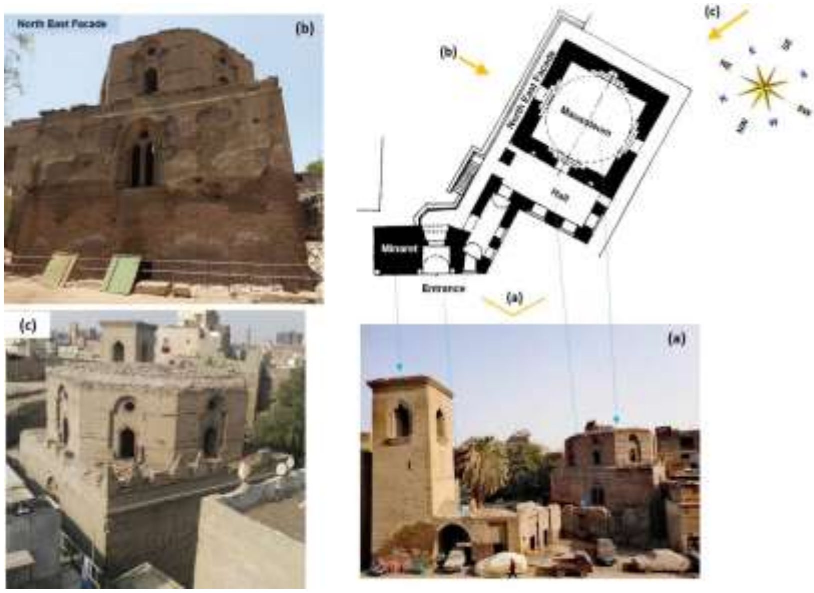


**Fig. 2.** Plan showing the mausoleum parts (modified after Rizk [27]) and three external photos: (a) northwest façade; (b) northeast façade; (c) southeast façade.

## Materials and Methods

### *Experimental programme*

The necessary samples were collected from the different construction materials and deterioration products, including the limestone, the old brick, the new brick, the mortar, and the crystallised salt. The experimental programme (Fig. 3) included measuring the physical properties of the bulk specific gravity, the water absorption, and the porosity of the limestone (five samples), the old brick (three samples), and the new brick (three samples). The petrographic analysis included two samples of the limestone, one sample of the old brick, and one sample of the new brick.

The chemical analyses consisted of XRD and SEM-EDX. The XRD examination considered two samples of each of the limestone, the mortar, and the salt, and one sample of each of the old brick and the new brick. Similarly, the SEM-EDX examination was performed on two samples of each of the limestone, the mortar, and the salt, and one sample of each of the old brick and the new brick. Finally, mechanical testing of the compressive strength was carried out on 15 samples. From the limestone, three cubes and three cylinders were tested. From the old brick and the new brick, six and three cubes were tested, respectively. In total, 43 samples were employed in all the examinations, analyses, and tests that were performed at the rock engineering laboratory of the Faculty of Engineering at Cairo University.

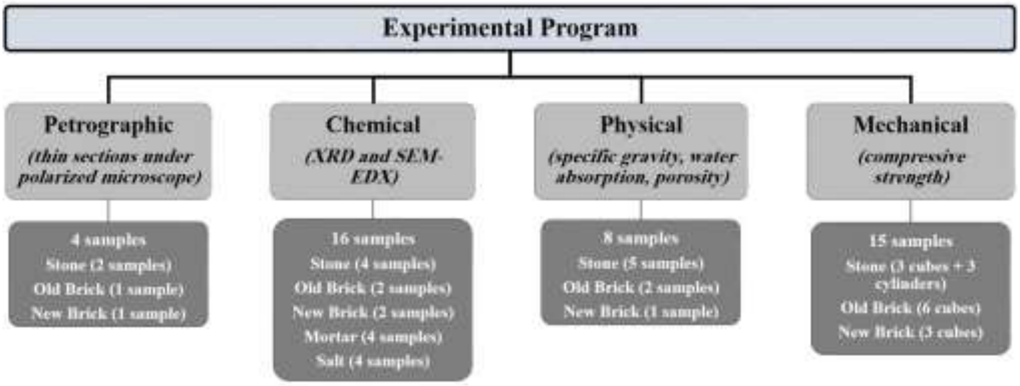


**Fig. 3.** Scheme of the implemented experimental programme: type of tests and number of samples in each test

### *Petrographic investigation*

The thin sections of the limestone samples, the old brick, and the new brick were prepared and then investigated using the polarised microscope. Figure 4 shows the photomicrograph of the first examined lime-stone thin section [(a) to (c)] and the second examined thin section [(d) to (f)].'=

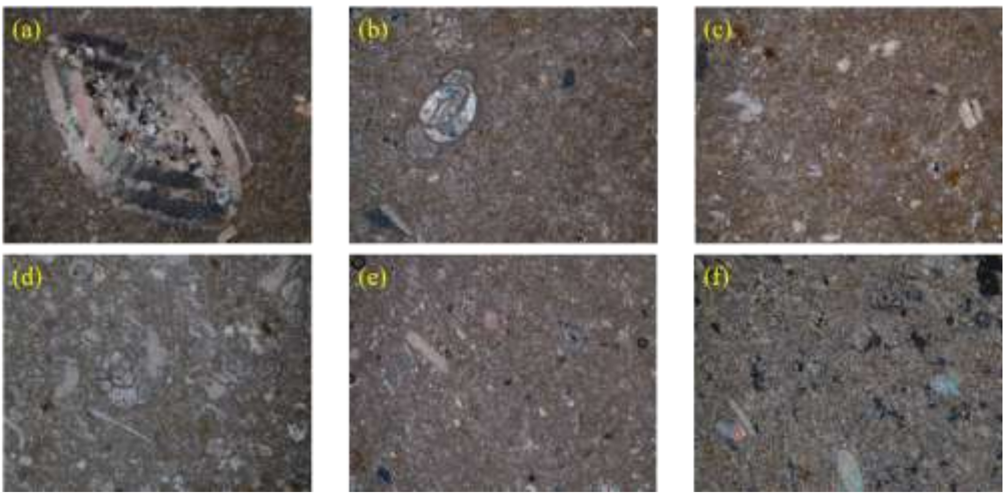


**Fig. 4.** Thin sections of the limestone under a polarised microscope: sample (1) from (a) to (c), and sample (2) from (d) to (f). Magnification: 5× for a, b, c, and d; 10× for d and e.

The first limestone thin section showed nummulitic and fossiliferous wackstone microfacies with Nummulites sp. It had very little dissolved Sparry calcite on the shell of the nummulite grain (Fig. 4a). Miliolids appeared floating in the dense micritic matrix (Fig. 4-b), and small fragments of echinoids and small benthic foraminifera of textulariids floated in the dense micritic matrix. A few microsparite-pseudosparrite crystals were present in the groundmass (Fig. 4c). In addition, the groundmass showed compaction with yellowish-brown clays within the matrix (Figs. 4b and c).

The second limestone thin section showed fossiliferous wackestone to packstone microfacies. It showed echinoid spines, echinoid fragments, miliolids, and textulariids (Fig. 4d). Microsparrite-pseudosparrite cement occurred within the groundmass (Fig. 4e). A few pores were either present as fractures or after the dissolution of the Sparry calcite cement (Fig. 4f).

The old brick thin section under the polarised microscope showed concretions of carbonates or clays floating in the clay cement (Fig. 5a). Some of the concretions had detrital quartz grains (Fig. 5b). Highly dissolved concretions appeared with few quartz grains (Fig. 5c). Spheroidal concretions appeared in point-contact packing with porosity (Fig. 5d). High porosity was detected in the dissolved concretions (Fig. 5e and f).

The photomicrograph of the new brick thin section appeared to have sub-rounded to subangular, monocrystal-line quartz grains (Figs. 6a and b) and elongated to prismatic plagioclase feldspars (Figs. 6c and d). The fresh and clear feldspars without alteration were noticed. Some of the detrital grains were muscovite (Fig. 6e), besides being clay cement. Few iron oxides occurred as concretions, leaving pores between them and the clay cement (Fig. 6f). All the photomicrographs showed absence or very few pores with well-arranged grains.

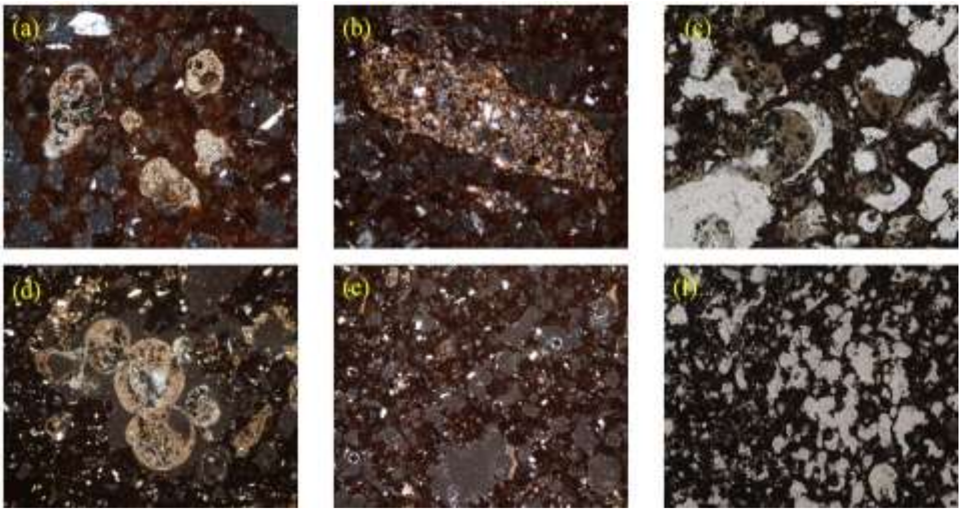


**Fig. 5.** hin sections of the old brick under a polarised microscope.
Magnification: 5× for d, e, and f; 10× for a, b, and c

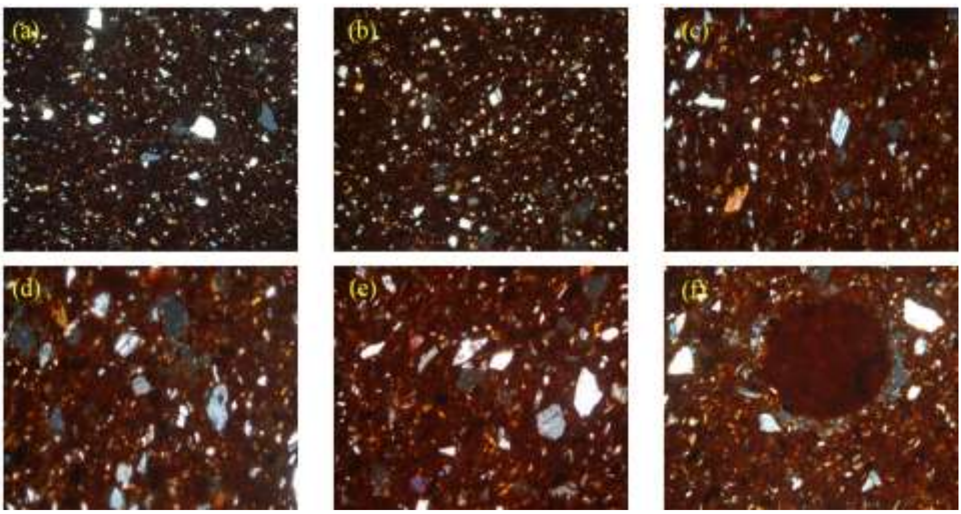


**Fig. 6.** Thin sections of the new brick under a polarised microscope.
Magnification: 5x for a, and b; 10 x for c, d, e and f.

***Chemical analysis***

The thin sections of the samples of limestone, the old brick, and the new brick were prepared and then investigated using the polarised microscope. Figure 4 shows the photomicrograph of the first examined lime-stone thin section [(a) to (c)] and the second thin section examined [(d) to (f)].

*XRD*

The XRD analysis showed that the used stone is limestone composed of calcite (CaCO3) with a limited amount of dolomite, quartz (SiO2), and the salt of halite (NaCl), figure 7a. The salt appeared due to its penetration into the groundwater in the limestone masonry walls by the capillary rise. Table 1 summarises the obtained weight percentages of each of the examined materials: the limestone, the old brick, the new brick, the mortar, and the salt. It can be noticed that there is a limited amount of quartz (3% and 7%) and the salt of halite (3% and 6%) in the two analysed samples of the limestone.

**Table 1.** Chemical decomposition of the different samples.

| Sample | Mineral Name | Chemical Formula | Semi-Quant [%] |
|---|---|---|---|
| Limestone-1 | Calcite, magnesium | $(Mg_{0.06} – Ca_{0.94}) (CO_3)$ | 87 |
| | Halite | NaCl | 6 |
| | Quartz | $SiO_2$ | 7 |
| Limestone-2 | Calcite, magnesian | $(Mg_{0.064}\ Ca_{0.936})\ (C\ O_3)$ | 95 |
| | Quartz | $SiO_2$ | 3 |
| | Halite | NaCl | 2 |
| Old brick | Quartz | $SiO_2$ | 40 |
| | Halite | NaCl | 10 |
| | Liottite | $(Na_{9.96}\ K_{6.04}\ Ca_2)\ Ca_6\ (Si_{18}\ Al_{18}\ O_{72})\ (SO_4)\ 5\ Cl_{3.5}\ F_{0.5}$ | 20 |
| | Albite, calcian | $(Na_{0.84}\ Ca_{0.16})\ Al_{1.16}\ Si_{2.84}\ O_8$ | 30 |
| New brick | Quartz | $SiO_2$ | 60 |
| | Halite | NaCl | 5 |
| | Albite, calcian | $(Na, Ca)\ Al\ (Si, Al)_3\ O_8$ | 30 |
| | Wadalite | $Ca_{12}\ Al_{10.6}\ Si_{3.4}\ O_{32}\ Cl_{5.4}$ | 5 |
| Mortar-1 | Halite | NaCl | 72 |
| | Calcite | $Ca\ CO_3$ | 25 |
| | Quartz | $SiO_2$ | 3 |
| Mortar-2 | Halite | NaCl | 62 |
| | Calcite | $Ca\ (CO_3)$ | 23 |
| | Quartz | $SiO_2$ | 15 |
| Salt-1 | Halite | NaCl | 75 |
| | Quartz | $SiO_2$ | 6 |
| | Kyanite | $Al_2\ SiO_5$ | 19 |
| Salt-2 | Halite | NaCl | 80 |
| | Quartz | $SiO_2$ | 3 |
| | Kyanite | $Al_2\ SiO_5$ | 17 |

The old brick analysis showed that it had a high percent of the silica minerals represented in quartz (40%), albite (30%), and liottite (20%) (Table 1 and Figure 7a). It had a high percent of halite salt (10%), again due to its penetration into the walls by the capillary rise.

The new brick seemed compatible with the old one to a good extent. It also had a high percent of the silica minerals represented in quartz (60%), albite (30%), and wadalite (5%), as shown in Table 1 and Figure 7b. It had a lower percent of halite salt (5%) compared with the old brick. This could be attributed to its lower porosity and water absorption compared with the old brick, as will be discussed later.

The mortar found to be composed of lime represented in calcite appeared with 25% and 23% mixed with sand represented in quartz with 3% and 15% (Table 1 and Figure 7d). The high percentage of halite (72% and 62%) confirmed the high level of deterioration caused by the salt penetration in the mortar joints. The salt analysis indicated that it was halite (75% and 80%). It was found mixed with some silica minerals in the quartz, and the kyanite resulted from the building materials themselves (Table 1 and Figure 7e).

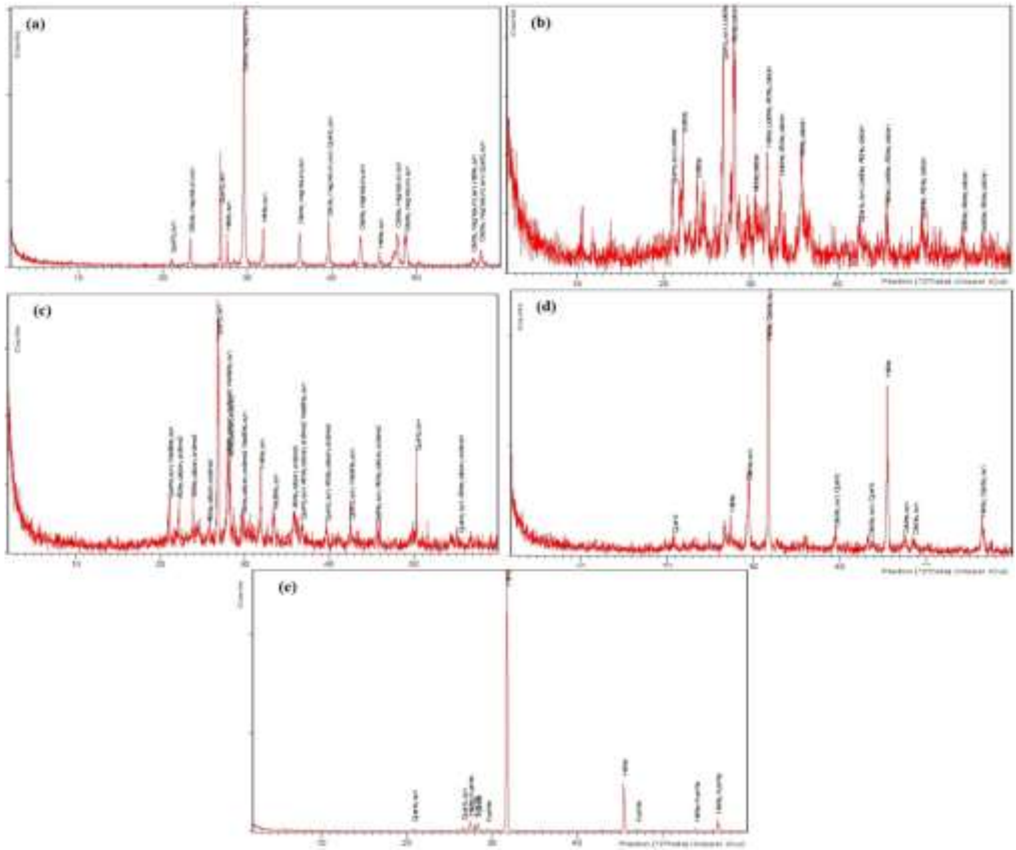

**Fig. 7.** XRD spectra: (a) limestone; (b) old brick; (c) new brick; (d) mortar; (e) salt.

*SEM-EDX*

The investigation of the limestone samples under the SEM showed that it had voids, high porosity, and a lack of cohesion between the constituents (Figs. 8a and b). This occurred due to the deterioration of the limestone. The silica and dolomite particles and clay minerals were noticed between the calcite particles of the limestone. Some halite salt was found precipitated between the limestone particles.

The limestone's primary constituting elements were Ca, C, O, and Si, according to the EDX study (Fig. 9). The weight percent containing the elements Ca, C, O, and Si ranged from (14.6:26.0), (8.1:11.6), (16.1:42.8), and (1.4:6.4), respectively, in the two limestone samples under examination (LS-1 and LS-2). The elements Na (1.7:23.5), Cl (4.7:29.7), S (1.2:3), and K (1.7:3.3) all contributed to the existence of salts.

The old brick investigation showed good manufacturing practise as the components of the brick were well incorporated. However, due to the weathering effects, voids were noticed, and halite was found (Fig. 8c). For the new brick, the voids between the particles and the disintegration between the constituents were noticed. The halite salt was identified (Fig. 8d).

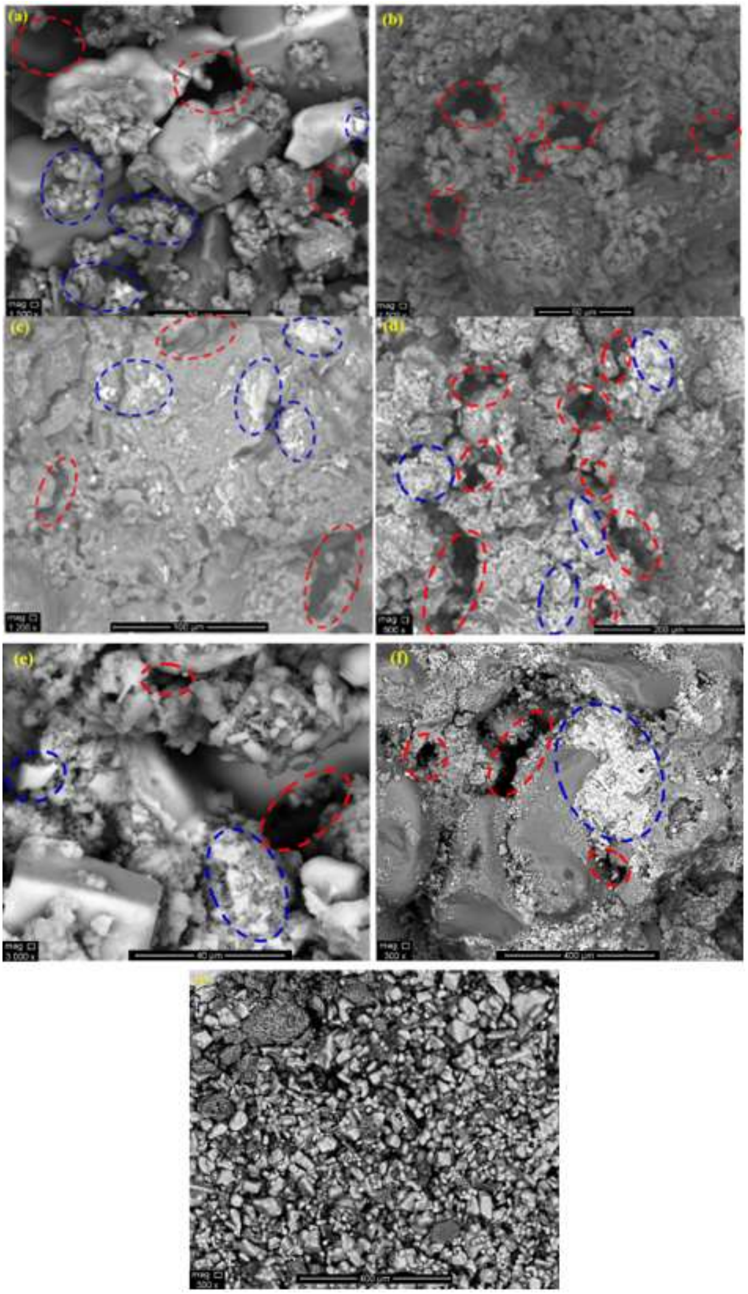

**Fig. 8.** SEM images: (a) limestone sample-1; (b) limestone sample-2; (c) old brick; (d) new brick; (e) mortar sample-1; (f) mortar sample-2; (g) salt sample. Red shapes indicate voids, and blue shapes indicate salts.

The EDX analysis (Fig. 9) showed the high presence of silica in the old brick. In the examined sample, the weight percent existence of the elements was Si (17.3:26.8), Ca (5.5:18.1), Al (0:10.3), Ti (1.2:1.8), Fe (12.6:15.7), K (0.7:1.7), and Mg (2.2:3.4). The salts existence existed in the existence of Na (0:2.7), Cl (0:0.5), and Br (0:10.7). Similarly, the new brick had a high silica content. In the examined sample, the weight percent existence of the elements was Si (6.2:22.2), Ca (2.1:6), Al (2.3:8.9), Ti (0:1.4), Fe (2.4:8.6), K (1.8:3.5), and Mg (0:2.2). Again, the salts appeared in the presence of Na (3.4:26.5) and Cl (4.8:46.2).

The SEM images of the mortar showed the high salt concentration and the weak composition of the binding material due to moisture effects and salt crystallisation (Figs. 8-e and f). The EDX analysis confirmed the XRD results that the mortar contained a high percent of salts, as high weight percents of Na (up to 31), Cl (up to 69), and S (0:20.7) were found. The samples contained high percentages of Ca (up to 36.9), Si (up to 25.6), O (up to 36.8), and C (up to 11.4), reflecting the nature of mortar as a lime-based one (Fig. 9). The salt investigation revealed that it was halite (NaCl) with cubic crystals (Fig. 8g). The EDX analysis found the weight percentages of Na (up to 36) and Cl (up to 54.8).

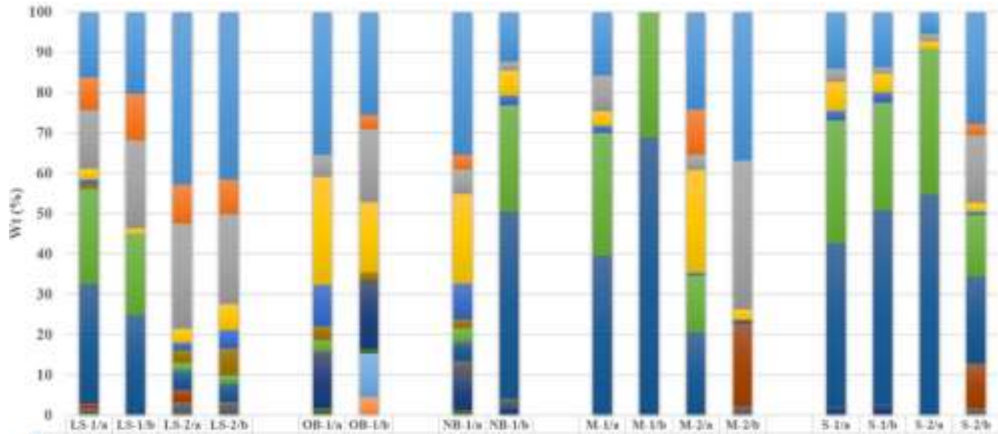


| | LS-1/a | LS-1/b | LS-2/a | LS-2/b | OB-1/a | OB-1/b | NB-1/a | NB-1/b | M-1/a | M-1/b | M-2/a | M-2/b | S-1/a | S-1/b | S-2/a | S-2/b |
|---|---|---|---|---|---|---|---|---|---|---|---|---|---|---|---|---|
| O | 16.1 | 20.2 | 42.8 | 41.5 | 35.4 | 25.5 | 35.3 | 12.4 | 15.7 | 0.0 | 24.1 | 36.8 | 14.1 | 13.7 | 5.5 | 27.7 |
| C | 8.1 | 11.6 | 9.7 | 8.7 | 0.0 | 3.5 | 3.7 | 0.0 | 0.0 | 0.0 | 11.4 | 0.0 | 0.0 | 0.0 | 0.0 | 2.9 |
| Ca | 14.6 | 21.9 | 26.0 | 22.3 | 5.5 | 18.1 | 6.0 | 2.1 | 8.9 | 0.0 | 3.6 | 36.9 | 3.3 | 1.7 | 1.8 | 16.6 |
| Si | 2.6 | 1.4 | 3.4 | 6.4 | 26.8 | 17.3 | 22.2 | 6.2 | 3.6 | 0.0 | 25.6 | 2.7 | 7.1 | 4.7 | 1.9 | 2.2 |
| Al | 1.4 | 0.0 | 1.9 | 4.4 | 10.3 | 0.0 | 8.9 | 2.3 | 1.7 | 0.0 | 0.5 | 0.0 | 2.4 | 2.4 | 0.0 | 6.8 |
| Mg | 1.0 | 0.0 | 3.3 | 6.7 | 3.4 | 2.2 | 2.2 | 0.0 | 0.0 | 0.0 | 0.0 | 0.0 | 0.0 | 0.0 | 0.0 | 0.0 |
| Na | 23.5 | 20.0 | 1.7 | 2.0 | 2.7 | 0.0 | 3.4 | 26.5 | 30.4 | 31.0 | 14.2 | 0.0 | 30.5 | 26.7 | 36.0 | 15.3 |
| Cl | 29.7 | 24.9 | 4.9 | 4.7 | 0.0 | 0.5 | 4.8 | 46.2 | 39.7 | 69.0 | 20.6 | 0.7 | 40.4 | 48.0 | 54.8 | 21.5 |
| S | 1.2 | 0.0 | 3.0 | 0.0 | 0.0 | 0.0 | 0.0 | 0.0 | 0.0 | 0.0 | 0.0 | 20.7 | 0.0 | 0.0 | 0.0 | 11.2 |
| K | 1.7 | 0.0 | 3.3 | 3.3 | 1.7 | 0.7 | 3.5 | 1.8 | 0.0 | 0.0 | 0.0 | 2.2 | 0.0 | 0.0 | 0.0 | 1.7 |
| Fe | 0.0 | 0.0 | 0.0 | 0.0 | 12.6 | 15.7 | 8.6 | 2.4 | 0.0 | 0.0 | 0.0 | 0.0 | 2.3 | 2.9 | 0.0 | 0.0 |
| Ti | 0.0 | 0.0 | 0.0 | 0.0 | 1.8 | 1.2 | 1.4 | 0.0 | 0.0 | 0.0 | 0.0 | 0.0 | 0.0 | 0.0 | 0.0 | 0.0 |
| Br | 0.0 | 0.0 | 0.0 | 0.0 | 0.0 | 10.7 | 0.0 | 0.0 | 0.0 | 0.0 | 0.0 | 0.0 | 0.0 | 0.0 | 0.0 | 0.0 |
| P | 0.0 | 0.0 | 0.0 | 0.0 | 0.0 | 4.7 | 0.0 | 0.0 | 0.0 | 0.0 | 0.0 | 0.0 | 0.0 | 0.0 | 0.0 | 0.0 |

**Fig. 9.** The weight percent (Wt%) found for each element in each sample (LS: limestone, OB: old brick, NB: new brick, M: mortar, and S: salt) (a and b: the EDX spots in the analysed sample).

### *Physical testing*

The tests of the limestone were carried out following the ASTM standard C97/C97M-18 [30], and for the bricks, the ASTM standard C67/C67M-20 [31, 32] was followed. The collected limestone samples were prepared in either cubes with a length of 50mm or cylinders with a diameter of 44mm and a height of 88mm (Figure 10). The old brick and the new brick samples were prepared in cubes with a length of 50mm (Figure 10). Table 2 summarises the obtained results.

For the physical properties of the limestone, it was noticed that regardless of the sample shape, near values were obtained for the measured quantities. The bulk specific gravity was on average 2.03, with a low standard deviation of 0.04. The average water absorption was 8.15 with a low standard deviation of 0.74. The porosity was on average 7.53, with a low standard deviation of 0.63.

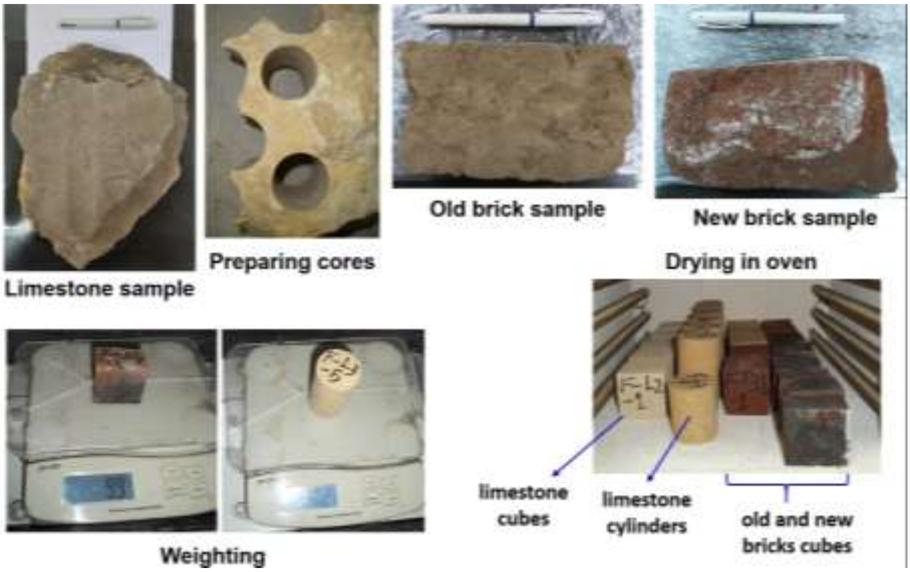


**Fig. 10.** Different photographs depict various raw samples, preparations, and tests.

**Table 2.** Chemical decomposition of the different samples

| Sample Code / Shape | Bulk Specific Gravity | Water Absorption (%) | Porosity (%) |
|---|---|---|---|
| | Limestone | | |
| F-L2-1 / cube | 1.99 | 9.23 | 8.45 |
| F-L2-5 / cube | 2.05 | 7.67 | 7.12 |
| F-L3-4 / cylinder | 2.09 | 7.29 | 6.80 |
| F-L3-5 / cylinder | 2.02 | 8.30 | 7.67 |
| F-L3-6 / cylinder | 2.02 | 8.24 | 7.62 |
| Average | 2.03 | 8.15 | 7.53 |
| Standard Deviation | 0.04 | 0.74 | 0.63 |
| | Old brick | | |
| F-BO3-1/cube | 1.10 | 16.16 | 13.91 |
| F-BO4-1/cube | 1.07 | 17.71 | 15.04 |
| Average | 1.09 | 16.94 | 14.48 |
| Standard Deviation | 0.02 | 1.10 | 0.80 |
| | New brick | | |
| F-B1-2/cube | 1.73 | 14.22 | 12.45 |

A comparison was made with the previous studies in which limestone samples were extracted and tested. These studies were found to be relatively limited. The limestone specimens were extracted from either the quarries utilised to build the historic structures in Cairo, namely Helwan, Mokkatam, or Tura. In addition, the results of specimens extracted from some other historic structures in Historic Cairo were considered, specifically the mosques of Al-Azhar and Sharf Al-Din, the mausoleum of Al-Imam Al-Shafi'I, the Sebil of Shahin Aga, Wekalat Al-Ghouri, and the Ayyubid City wall. The comparisons were plotted for the bulk specific gravity (Fig. 11), the water absorption (Fig. 12), and the porosity (Fig. 13). As can be noticed, the obtained results are comparable with the literature for the three physical properties.

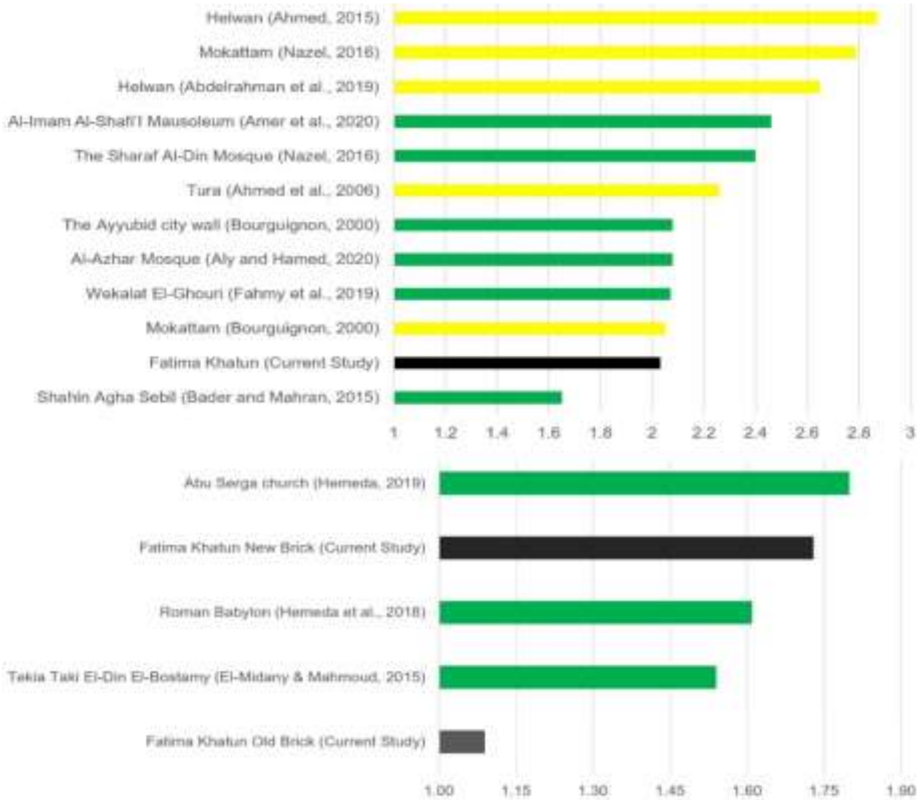


**Fig. 11.** Comparison of the bulk specific gravity (-) with the literature for the limestone (top) and the brick (bottom).


**Fig. 12.** Comparison of the water absorption (%) with the literature for the limestone (top) and the brick (bottom).

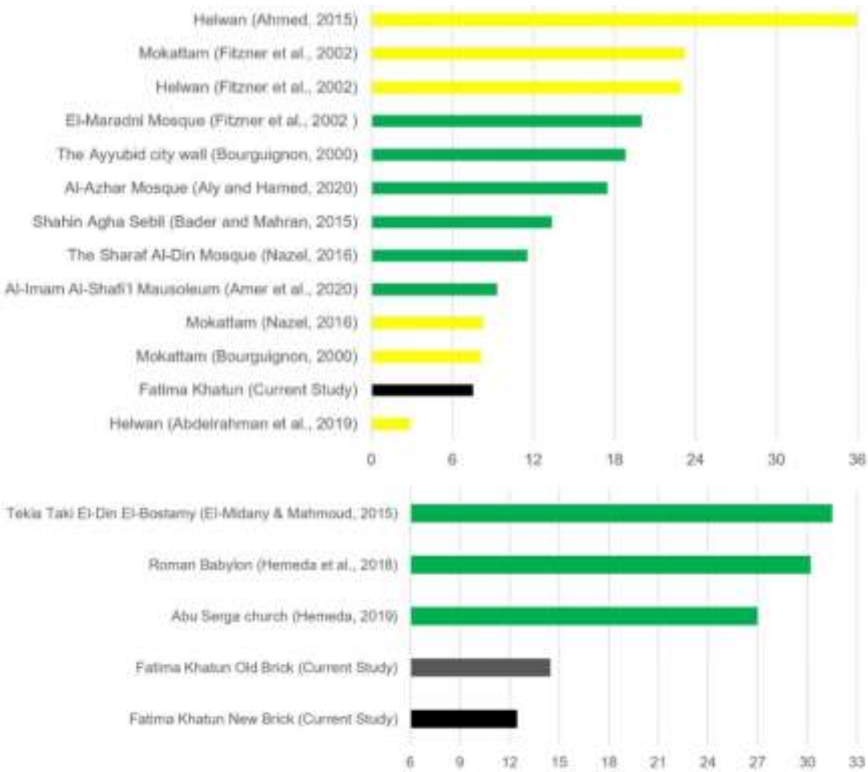


**Fig. 13.** Comparison of the porosity (%) with the literature for the limestone (top) and the brick (bottom).

### *Mechanical testing*

The compression test was carried out on three cylinders of limestone having a diameter and height of 44 and 88mm, respectively, and three cubes with a length of 50mm. For the old and the new brick, cubes with a length of 50mm were employed. One limestone cylinder failed in shearing along one plane (Fig. 14, top-left), and two samples failed in axial splitting (Fig. 14, top-middle and right). The limestone cubes failed in axial splitting. Table 3 summarises the obtained results. As can be noticed, the limestone cylindrical samples showed near-record results with an average of 10.53MPa and a relatively low coefficient of variation (CV) of 4.7%. The cube samples gave, as expected, a higher compressive strength of an average 17.15MPa with an acceptable CV of 17%. The higher strength of the cubes compared with the cylinders is a common observation in compression tests. It has to do with the friction that resulted between the sample's top and bottom surfaces and the machine's upper and lower caps. This friction gives the sample a sort of confinement. The effect is more pronounced when the sample is smaller. This is the case with the cube compared with the cylinder, which has 50 and 88 mm of height, respectively.

The new brick had almost three times the compressive strength of the old brick (15.75 MPa compared to 5.48 MPa). Also, the CV was lower (20.6% compared to 35.9%). The old brick showed axial splitting failure mode (Fig. 14, middle), whereas the new brick was crushed into coarse to fine powder (Fig. 14, bottom). The advanced state of deterioration of the old brick contributed notably to its showing such a mode of failure and low compressive strength.

**Fig. 14.** Failure of the samples in the compressive strength test:
The limestone (top), the new brick (bottom), and the old brick (bottom)

**Table 3.** Experimental observations on the tested limestone and brick samples.

| Sample Code | Shape | Compressive Strength (MPa) | Failure Mode |
|---|---|---|---|
| | | Limestone | |
| F-L2-2 | Cube | 15.54 | Axial splitting |
| F-L2-3 | Cube | 20.51 | Axial splitting |
| F-L2-4 | Cube | 15.40 | Axial splitting |
| Average | | 17.15 | SD = 2.91 CV = 17.0% |
| F-L3-1 | Cylinder | 10.07 | Shearing along single plane |
| F-L3-2 | Cylinder | 10.49 | Axial splitting |
| F-L3-3 | Cylinder | 11.05 | Axial splitting |
| Average | | 10.53 | SD = 0.49 CV = 4.7% |
| | | New brick | |
| F-B1-1 | Cube | 19.42 | Axial splitting |
| F-B2-1 | Cube | 13.25 | Axial splitting |
| F-B3-1 | Cube | 14.59 | Axial splitting |
| Average | | 15.75 | SD = 3.25 CV = 20.6% |
| | | Old brick | |
| F-BO1-1 | Cube | 3.26 | Crushing into fine to coarse powder |
| F-BO1-2 | Cube | 7.65 | Crushing into fine to coarse powder |
| F-BO2-1 | Cube | 2.94 | Crushing into fine to coarse powder |
| F-BO2-2 | Cube | 6.20 | Crushing into fine to coarse powder |
| F-BO3-2 | Cube | 7.15 | Crushing into fine to coarse powder |
| F-BO4-2 | Cube | 5.67 | Crushing into fine to coarse powder |
| Average | | 5.48 | SD = 1.97 CV = 35.9% |

A comparison is given between the obtained compressive strengths of the limestone and the brick with the available literature (Figure 15).

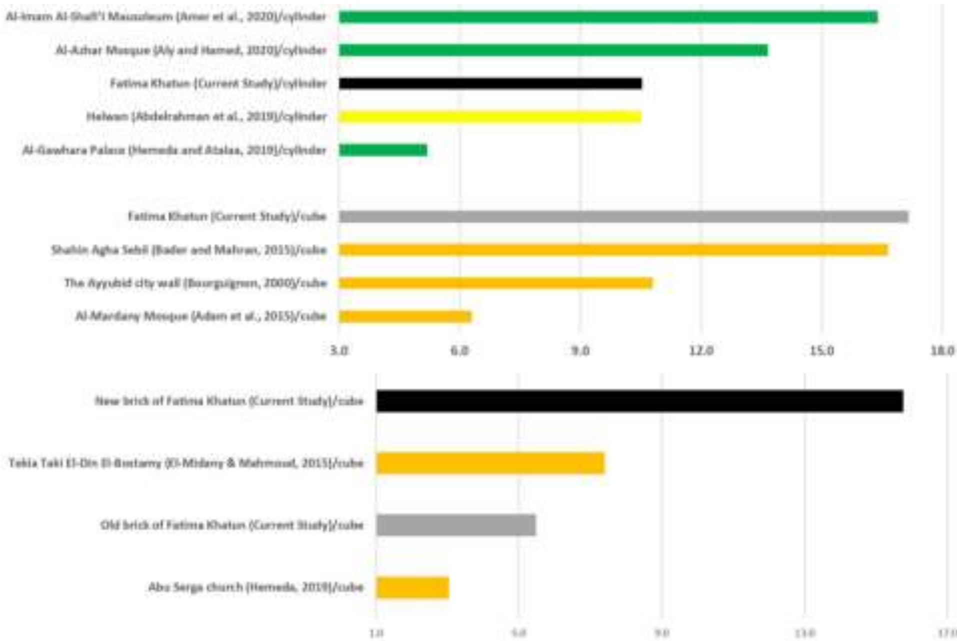


**Fig. 15.** Comparison of the compressive strength (MPa) with the literature for the limestone (top) and the brick (bottom)

Limestone cylinders were tested from three historic structures in Historic Cairo, namely: Al-Imam Al-Shafi'I mausoleum, Al-Azhar Mosque, and Al-Gawhara palace. In addition, samples from Helwan Quarry were tested. The obtained results for Fatima Khatun limestone showed comparable results. The same was observed with the limestone cubes, which showed comparable results with the tested samples from Shahin Agha Sebil, the Ayyubid city wall, and Al-Mardany mosque, all located in Historic Cairo. The old and the new brick showed again comparable results with the limited available literature of the two historic structures of Abu Serga Church and Tekia Taki El-Din El-Bostamy, both located in Historic Cairo.

## Conclusions

The paper presented an experimental programme aimed at the characterization of the construction materials of the Fatima Khatun Mausoleum (13th century) in historic Cairo. It has reached an advanced state of deterioration, and an urgent conservation plan is highly recommended.

The petrographic investigation of the limestone showed nummulitic and fossiliferous wackstone to packstone microfacies. The groundmass showed compaction and yellowish-brown clays within the matrix. A few pores were present as fractures. The old brick, due to its advanced state of degradation, showed high porosity in the dissolved concretions. The new brick showed fresh and clear feldspars without alteration and without or very few pores with well-arranged grains.

The XRD analysis showed that the limestone was composed of calcite with a limited amount of dolomite and quartz. The old brick was found to have a high percentage of the silica minerals represented in quartz, albite, and liottite. The new brick was found compatible in mineralogical composition with the old brick, with the same high percent of quartz and albite. Halite salt appeared in the limestone and the old brick due to its penetration into the walls by the capillary rise. The mortar was found to be composed of lime, represented in the calcite, mixed with sand, represented in the quartz. A high percentage of halite was detected in the mortar because of its high porosity.

The SEM analysis revealed that the limestone samples had voids, high porosity, and a lack of cohesion between their components, showing a high state of degradation. The old brick showed that, due to the weathering effects, voids were noticed and halite was found; nevertheless, the components of the brick were well incorporated, reflecting good old manufacturing practises. The mortar analysis revealed the weak composition of the binding materials and the high salt concentration, coinciding with the XRD findings.

The physical testing of the limestone (regardless of the sample shape, either cube or cylinder) showed a bulk specific gravity of 2.03 with a low CV. The water absorption and the porosity were 8.15 and 7.53, respectively, with a low CV. For the three physical properties, the obtained results were found to be comparable with other tested limestone samples from other historic structures in Historic Cairo. The old brick had a low specific gravity of only 1.09, whereas the new brick was heavier with a specific gravity of 1.73. In addition, the new brick was better than the old one in terms of water absorption (14.2 vs. 16.9) and porosity (12.5 vs. 14.5). Again, the results seem comparable with tested bricks from other historic structures in Historic Cairo, but for the old bricks, the specific gravity seemed clearly low.

The mechanical testing of the limestone samples in the form of cubes gave, as expected, higher compressive strength values than the cylindrical ones. The strengths of the cubes were about 60% higher than those of the cylinders. The new brick had almost three times higher compressive strength than the old brick (15.75MPa compared to 5.48MPa).

The characterization carried out for the construction materials of the Fatima Khatun Mausoleum gave a better understanding and will be employed in many ways. Regarding structural analysis, it is now possible to estimate the modulus of elasticity and the tensile strength and then carry out a sensitivity analysis on the estimated values. For conservation purposes, the chemical, petrographic, physical, and mechanical properties of the necessary limestone, brick, and mortar could now be selected with a higher level of knowledge to ensure the compatibility of the new materials with the historic ones.

## Acknowledgments

The study was carried out within the research project “Interdisciplinary approach for the management and conservation of UNESCO World Heritage Site of Historic Cairo - Application to Al-Ashraf Street” supported by Newton-Mosharafa funding program, a joint fund by Science, Technology, and Innovation Funding Authority (STIFA) of Egypt, Grant No. AHRC30799 and the Arts and Humanities Research Council (AHRC) of the UK, Grant No. AH/R00787X/1.

## References

[1] H. Badawi, S.A. Mourad, *Observations from the 12 October 1992 Dahshour earthquake in Egypt*, **Natural Hazards, 10**, 1994, pp. 261-274.

[2] A. Abd al-Mun’im, **The glory of Islamic Architecture: A Mission of Conservation 2002-2006,** Ministry of Culture, Cairo, Egypt, 2006.

[3] D.A. Saad, A. Elyamani, M.H. Moddather, S. Mourad, A Fund-Allocation *Optimization Framework for Prioritizing Historic Structures’ Conservation Projects - An Application to Historic Cairo*, **Proceedings of Canadian Society of Civil Engineers Annual Conference**, Laval, 12-15 June 2019, CON46-1-CON46-10.

[4] A. Elghazouli, A. Butler, S. Mourad, C. Cheeseman, **Interdisciplinary Approach for the Management and Conservation of UNESCO World Heritage Site of Historic Cairo. Application to Al-Ashraf Street,** UK Research and Innovation, 2018.

[5] A. Elyamani, P. Roca, *A review on the study of historical structures using integrated investigation activities for seismic safety assessment. Part I: dynamic investigation*, **Scientific Culture, 4**(l), 2018, pp. 1-27.

[6] A. Elyamani, P. Roca, *A review on the study of historical structures using integrated investigation activities for seismic safety assessment. Part II: model updating and seismic analysis,* **Scientific Culture, 4**(l), 2018, pp. 29-51. DOI: 10.5281/zenodo.1048243.

[7] L. Binda, L. Cantini, C. Tedeschi, *Diagnosis of Historic Masonry Structures Using Non-Destructive Techniques*, **Nondestructive Testing of Materials and Structures** (Editors: O. Güneş and Y. Akkaya)**,** RILEM Bookseries, vol 6, Springer, Dordrecht, 2013.

[8] * * *, *RILEM Recommendation MDT. D.5 - in-situ stress-strain behaviour tests based on the flat jack*, **Materials and Structures**, 37, 2004, pp. 497–501.

[9] E. Manning, L.F. Ramos, F.M. Fernandes, *Tube-Jack Testing for Irregular Masonry Walls: Regular Masonry Wall Testing*, **Journal of Nondestructive Evaluation, 35**, 2016, Article Number: 43.

[10] L. Pelà, E. Canella, A. Aprile, P. Roca, *Compression test of masonry core samples extracted from existing brickwork,* **Construction and Building Materials, 119**, 2016, pp. 230-240.

[11] D.V. Bompa, A.Y. Elghazouli, *Experimental and numerical assessment of the shear behaviour of lime mortar clay brick masonry triplets*, **Construction and Building Materials, 262,** 2020, Article Number: 120571.

[12] D.V. Bompa, A.Y. Elghazouli, *Compressive behaviour of fired-clay brick and lime mortar masonry components in dry and wet conditions*, **Materials and Structures, 53**, 2020, pp. 1-21.

[13] L. Binda, M. Lualdi, A. Saisi, L. Zanzi, *Radar investigation as a complementary tool for the diagnosis of historic masonry buildings*, **International Journal of Materials and Structural Integrity, 5,** 2011, pp. 1 - 25. DOI: 10.1504/IJMSI.2011.039043.

[14] S. Santos-Assunçao, V. Perez-Gracia, O. Caselles, J. Clapes, V. Salinas, *Assessment of Complex Masonry Structures with GPR Compared to Other Non-Destructive Testing Studies*, **Remote Sensing, 6**, 2014, pp. 8220-8237.

[15] E. Vasanelli, A. Calia, V. Luprano, F. Micelli, *Ultrasonic pulse velocity test for non-destructive investigations of historical masonries: an experimental study of the effect of frequency and applied load on the response of a limestone,* **Materials and Structures, 50**, 2017, Article Number: 38.

[16] A. Elyamani, O. Caselles, P. Roca, J. Clapes, *Integrated dynamic and thermography investigation of Mallorca cathedral*, **Mediterranean Archaeology and Archaeometry, 18**(1), 2018, pp. 221-236.

[17] P. Maravelaki-Kalaitzaki, A. Bakolas, I. Karatasios, V. Kilikoglou, *Hydraulic lime mortars for the restoration of historic masonry in Crete,* **Cement and Concrete Research, 35**(8), 2005, pp. 1577-1586.

[18] Y. Waseda, E. Matsubara, K. Shinoda, **X-Ray Diffraction Crystallography: Introduction, Examples and Solved Problems,** Springer Science & Business Media, 2011.

[19] S. Abdelaal, R. Yamani, M. Abdel-Fatah, I.G. Sandu, *Salt Weathering of Imni Tomb. Problem Identification and Characterization,* **International Journal of Conservation Science, 10**(4), 2019, pp. 661-680.

[20] P. López-Arce, E. Doehne, J. Greenshields, D. Benavente, D. Young, *Treatment of rising damp and salt decay: the historic masonry buildings of Adelaide, South Australia*, **Materials and Structures, 42**(6), 2009, pp. 827-848.

[21] J. Elsen, *Microscopy of historic mortars - A review*, **Cement and Concrete Research, 36**(8), 2006, pp. 1416-1424.

[22] V. Pelin, I. Sandu, S. Gurlui, M. Brinzila, V. Vasilache, I.G. Sandu, *Evaluation of the Artificial Aging Rate Through UV Radiation Exposure of Indigenous Carbonate Rocks, Treated with Water-solvated Nano-dispersions, with the Interest of Consolidation and the Formation of a Waterproof Character*, **Revista de Chimie, 67**(12), 2016, pp. 2568-2572.
[23] I. Sandu, *Modern Aspects Regarding the Conservation of Cultural Heritage Artifacts*, **International Journal of Conservation Science, 13**(4), 2022, pp. 1187-1208.
[24] F. Aras, G. Altay, *Investigation of mechanical properties of masonry in historic buildings*, **Gradevinar, 67**(5), 2015, pp. 461-469.
[25] C. Sabbioni, G. Zappia, C. Riontino, M. T. Blanco-Varela, J. Aguilera, F. Puertas, E.E. Toumbakari, *Atmospheric deterioration of ancient and modern hydraulic mortars*, **Atmospheric Environment, 35**(3), 2011, pp. 539-548.
[26] K.A.C. Creswell, **Papers and Photograph Collection of Islamic Architecture,** Rare Books and Spe-cial Collections Library, A 19 Pl 6 A/4 American University in Cairo.
[27] A.M. Rizk, **Atlas Al-‘imara Al-islamiyya wa’l-qibtiyya bi’l-Qahira**, vol. 2, Cairo, 2002.
[28] S.M. Maher, **Masajid Misr wa-’awliya’uha Al-Salihun**, vol. 3, Cairo, 1983.
[29] * * *, **The Bulletins of the Comité de Conservation des Monuments de l’Art Arabe, Group 18,** 1904, Comite Bulletin, Engineering Report No. 292, pp. 113.
[30] * * *, **Standard Test Methods for Absorption and Bulk Specific Gravity of Dimension Stone**, ASTM C97/C97M-18, ASTM International, 2018.
[31] * * *, **Standard Test Methods for Sampling and Testing Brick and Structural Clay Tile,** ASTM C67/C67M-20, ASTM International, West Conshohocken, PA, 2020.
[32] * * *, **Egyptian Code for Design and Construction of Masonry Works**, ECP-204, Housing and Building National Research Center, Cairo, Egypt, 2005.

*Received: April 16, 2022*
*Accepted: March 20, 2023*